1. Supplementary Information

1.1. Blood flow computations

Microcirculatory blood flow is modeled as a biphasic suspension composed of a plasma phase and a red blood cell phase. The bulk flow estimations are given in this section, the drift flux computation for the uneven distribution of red blood cells in bifurcations has been described in the Methods section.

Due to the low Womersley numbers (Wo<0.1) in the microvessels, pulsatile motion of blood can be ignored. Additionally, low Reynolds numbers in the microcirculation (Re<1) permit neglecting inertia so that steady conditions may be assumed for bulk flow. The microcirculation is represented as a network of interconnected cylindrical vessel segments. Mass conservation is enforced by the continuity eq. 11. The hydrostatic blood pressure drop across a vessel, ΔP is the product of the bulk flow, *Q*, through the vessel and its vascular resistance, α. Each cylindrical vessel segment is assigned a hydraulic resistance approximated by the viscosity modified Poiseuille Law, described in eq. 12 which is a function of the dynamic viscosity of blood plasma, μ, and the vessel's length, L, radius, R, and the *in vivo* viscosity adjustment, η_{vivo}. The viscosity adjustment depends on vessel radius and discharge hematocrit[49-50]. The drift flux velocity between the plasma and RBCs is given in eq. 1-2 in the methods section. The bulk and hematocrit fields are solved iteratively until simultaneous convergence.

$$\vec{\nabla} \cdot Q = 0 \tag{11}$$

$$\Delta P = Q\alpha = Q \cdot \frac{8\mu L}{\pi R^4} \cdot \eta_{vivo}(R, H_d) \tag{12}$$

1.2. Nonlinear biphasic oxygen dissociation

Oxygen dissociation kinetics from oxygen bound on erythrocytes to the plasma was approximated as a first-order reversible reaction, shown in eq. 13. The oxygen dissociation reaction rate from the red blood cells to the plasma, $\dot{R}_{R\to P}$, is governed by the forward reaction rate constant, k_f, the backward dissociation reaction rate constant, k_b, the hematocrit, H_t, and the volume of the cylindrical blood vessel segment, V_b.

$$\dot{R}_{R\to P} = H_t V_b\left(k_f C_{HbO_2} - k_b C_{plO_2}\right) \tag{13}$$

By introducing the equilibrium constant, $K_{eq} = k_b/k_f$, the backward reaction rate constant can be eliminated as shown in eq. 14. The introduction of the equilibrium constant inot the dissociation kinetics guarantees the reaction rates obey the Hill equation at equilibrium.

$$\dot{R}_{R\to P} = H_t V_b k_f \left(C_{HbO_2} - K_{eq} C_{plO_2}\right) \tag{14}$$

The equilibrium constant is equal to the ratio of the freely dissolved plasma oxygen concentration, C_{plO_2}, under the bound oxygen concentration shown in eq. 15. The bound oxygen concentration is the product of the total oxygen carrying capacity of RBC, β, and the hemoglobin saturation, S. Hemoglobin saturation is a function of plasma oxygen tension, pO_2, defined as the product of the plasma free oxygen concentration and the Henry's solubility of oxygen in plasma, α_{pl}.

$$K_{eq} = \frac{\beta \cdot S\left(C_{plO_2} \cdot \alpha_{pl}\right)}{C_{plO_2}} \qquad S(pO_2) = \frac{1}{1 + (P_{50}/pO_2)^n} \tag{15}$$

The physiological equilibrium saturation of RBC is determined by the Hill equation[66,67], which describes hemoglobin saturation in terms of the oxygen tension at 50% oxygen saturation, P_{50}, and the Hill coefficient, *n*, defined in Table 2. A constant value of pH=7.4 was assumed.

1.3. Distribution of surface area for each data set

The distribution of vessel surface area between pial arteries, penetrating arterioles, capillaries, penetrating venules and pial veins was determined for each data set. The distribution of surface area to capillaries was over-represented in data set 2, and penetrating arterioles and venules were below standard deviation when compared to the average of all four data sets. Low blood flow and tissue perfusion were computed this second data set, indicating that these statistical morphological variations affect the microcirculatory hydraulic resistance.

Table 4 Percent surface area fraction

Data Set	Mouse 1	Mouse 2	Mouse 3	Mouse 4	Mean
Pial Arteries	2.6%	3.9%	3.6%	3.8%	3.5±0.5%
Penetrating Arterioles	1.3%	0.5%	1.9%	2.9%	1.6±0.9%
Capillaries	88.5%	93.1%	87.8%	87.1%	89.1±2.4%
Penetrating Venules	2.0%	0.8%	2.7%	2.4%	2.0±0.7%
Pial Veins	5.5%	1.7%	4.0%	3.9%	3.8±1.4%

1.4. Mesh Independence Investigation

This section demonstrates that computer predictions of the coupled hemodynamics and oxygen transport models were independent of mesh discretization. The edge length for the extravascular domain was gradually refined for each data set. The cylindrical vessel segments in the network were also refined so that the arc length of each vessel was commensurate with the edge length of the mesh. Predictions stabilized when edge length was in the order of 5-10μm as exemplified for total oxygen extraction shown in Figure 8. For the finest mesh resolution (6.6μm), more than 3 million equations had to be solved iteratively with an over-relaxed Gauss Seidel method requiring 14-24 CPU hours.

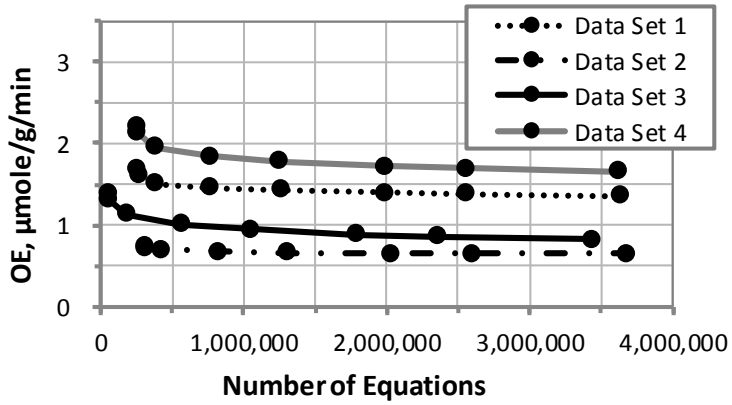

edge length	M1	M2	M4	M4
100, µm	0.5	0.6	0.5	0.1
50, µm	1.7	8.5	0.6	3.4
20, µm	3.3	13.7	2.4	8.9
12, µm	8.5	28.5	7.5	18.2
10, µm	13.4	3.6	3.5	33.0
8.3, µm	7.7	12.5	10.8	14.0
7.6, µm	10.0	10.0	16.1	11.6
6.6, µm	14.6	18.7	24.4	14.8

Figure 8. Mesh Independence Study. Oxygen extraction and profiles (data not shown) was computed for different edge lengths for each data set. In coarse meshes (50-100µm), oxygen extraction was sensitive to edge length. As the compuational domain for solving the reaction-diffusion equations was gradually refined, oxygen transport was no longer affected. For all four data sets mesh independence was achieved between 2.5-3.0 million equations corresponding to an approximate mesh edge length of 6.6µm.

1.5. Hierarchy of Hydraulic Resistance

The hydraulic conductivity as a function of branch order from the penetrating arteriole may be of interest in further determining the spatial distribution of resistance in the microcirculation. Each vessel within the capillary bed was assigned a minimum branch order based on the number of vessels traversed from its corresponding feeding penetrating arteriole. Should a vessel be connected by multiple paths to one or more penetrating arterioles (as is the case in the naturally anastomosed and highly interconnected capillary bed), the minimum order of branches to a penetrating arteriole was recorded. This categorization was limited as higher order capillaries could not be reliably categorized due to the multitude of feeding penetrators. As such, capillaries with branch order 7 or higher were excluded from the investigation.

Mean capillary diameter was plotted against branch order as shown in Figure 9A. Capillaries narrowed slightly as they increase in branching order, from 5µm at the first order branch to 4.1µm at the 4^{th} through 7^{th} order branches. This led to a corresponding increase in capillary hydraulic resistance as shown in Figure 9B. The average hydraulic resistance of capillaries connected to the feeding arteriole is nearly an order of magnitude lower than vessels with a branch order of 4^{th} or higher. Simultaneously, higher branch order capillaries also display a higher variance for both diameter and resistance. This analysis demonstrates that the capillary bed cannot be modeled as a collection of resistors arranged in series. The contributions of high order branches to overall capillary bed resistance are both significant and highly variable.

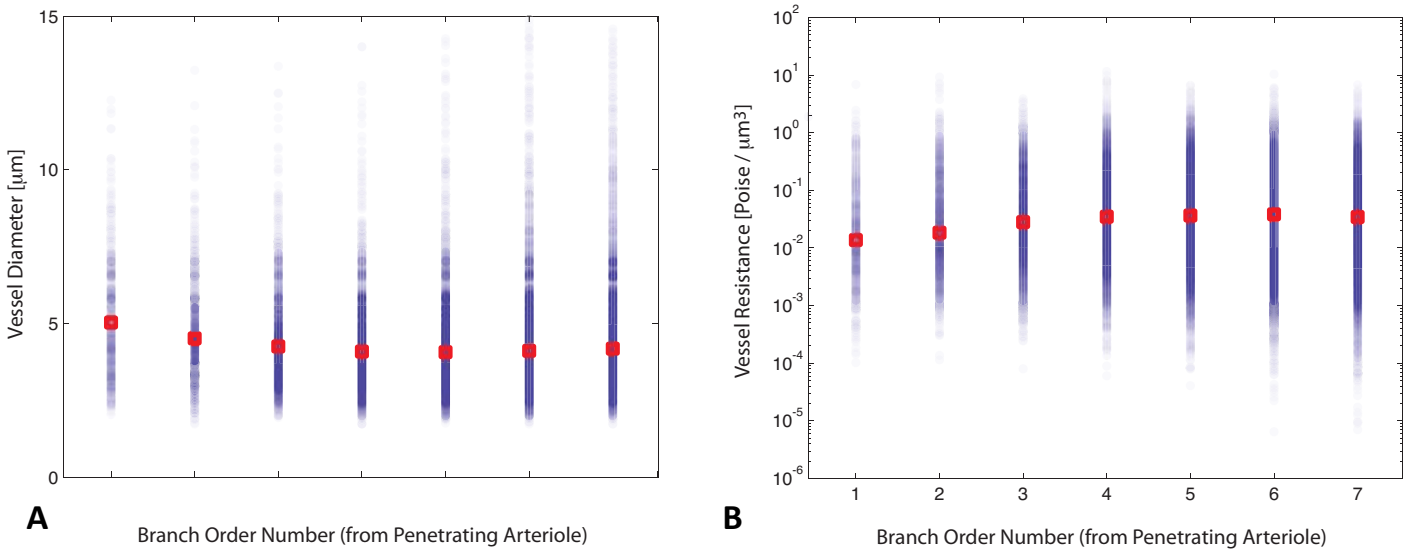

Figure 9. Morphological and hydraulic characteristics of the capillary bed as a function of branch order. Average values shown as a red box, distribution of values at each branch order shown in blue. **A.** Diameter of arterioles and capillaries as a function of branch order from the penetrating arteriole. The mean capillary diameter of 5µm decreases slightly with increasing branching order. **B.** Hydraulic resistance of individual vessels as a function of branch order. Mean capillary hydraulic resistance near the feeding arteriole is an order of magnitude lower than vessels with a branch order of 4th or higher.